

Free Vibration Analysis of Anisotropic Thin-Walled Closed-Section Beams

Erian A. Armanios*

Georgia Institute of Technology, Atlanta, Georgia 30332-0150
and

Ashraf M. Badir†

Clark Atlanta University, Atlanta, Georgia 30314

The equations of motion for the free vibration analysis of anisotropic thin-walled closed-section beams are derived using a variational asymptotic approach and Hamilton's principle. The analysis is applied to two laminated composite constructions. The circumferentially uniform stiffness produces extension-twist coupling and the circumferentially asymmetric stiffness produces bending-twist coupling. The effect of the elastic coupling mechanisms on the vibration behavior of thin-walled composite beams is evaluated analytically. The influence of stacking orientation on the frequencies associated with coupled vibration modes is investigated. The predictions are validated by comparison with a finite element simulation and test data.

Introduction

COMPOSITE designs offer the advantage of achieving favorable deformation modes through elastic tailoring. Structural coupling such as extension twist and bending twist are created as a result of the anisotropic properties of composite materials. Several theories have been developed for the analysis of thin-walled anisotropic beams. A review is presented in Ref. 1. Missing from this review is the work of Reissner and Tsai,² which is based on developing an exact solution to the governing equilibrium, compatibility and constitutive relationships of shell theory. A pertinent element in the analytical modeling development is the inclusion of the cross-sectional warping which allows the three-dimensional contributions to be recovered from a one-dimensional beam formulation. The major difference among the various theories lies in the methodology used to derive the warping of the cross section and include its contributions into a one-dimensional theory. The work of Refs. 3–9 uses the displacement field of classical thin-walled beam theory with shear deformation as the basis of its analytical development. In Refs. 4 and 5 a shear correction factor was introduced in order to reduce the overestimated bending stiffness. Shear stiffness correction factors were also proposed in the finite element formulation of Ref. 10. Local in-plane deformations and out-of-plane warping of the cross section were expressed in terms of unknown functions by Kosmatka.¹¹ These functions were assumed to be proportional to the axial strain, bending curvature, and twist rate and were determined using finite elements.

A variational asymptotic analysis was developed in Refs. 12 and 13 to derive the displacement field of anisotropic thin-walled closed-cross-sectional beams. In addition to the classical torsion-related warping, the derived displacement field includes out-of-plane warping due to uniform axial extension and bending as well. In the present paper, the theory of Refs. 12 and 13 is extended to the free vibration analysis of thin-walled anisotropic beams. An alternative approach is used to derive the out-of-plane warping function. The equations of motion and the associated boundary conditions are derived using Hamilton's principle.

To illustrate the influence of coupling on the vibration response, the theory is applied to two laminated composite configurations.

The first is the circumferentially uniform stiffness (CUS), which produces extension-twist coupling, whereas the second, the circumferentially asymmetric stiffness (CAS), produces bending-twist coupling.

Analytical Model

Consider the slender thin-walled elastic cylindrical shell shown in Fig. 1. The length of the shell is denoted by L , its thickness by h , the radius of curvature of the middle surface by R , and d represents a characteristic cross-sectional dimension. It is assumed that

$$d \ll L \quad h \ll d \quad h \ll R \quad (1)$$

It is also assumed that the variation of the material properties over distances of order d in the axial direction is small. The material is anisotropic, and its properties can vary circumferentially and in a direction normal to the middle surface as well. The shell thickness varies along the circumferential direction. Equations $y = y(s)$ and $z = z(s)$ define the closed contour Γ in the y, z plane associated with the Cartesian coordinate system x, y , and z shown in Fig. 1. The circumferential coordinate s is measured along the tangent to the middle surface in a counterclockwise direction.

The out-of-plane cross-sectional warping is derived by adding a correction function to the classical displacement field of extension, bending, and torsion of thin-walled beams. This correction function is shown to account for the contribution of the material's anisotropy in the displacement field.

Displacement Field

The displacement field is expressed as

$$\begin{aligned} u_1(x, s) &= U_1(x) - y(s)U_2'(x) - z(s)U_3'(x) + g(s, x) \\ u_2(x, s) &= U_2(x) - z(s)\varphi(x) \\ u_3(x, s) &= U_3(x) + y(s)\varphi(x) \end{aligned} \quad (2)$$

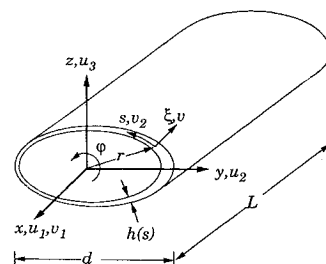


Fig. 1 Coordinate systems and kinematic variables.

Received Feb. 15, 1994; revision received Jan. 14, 1995; accepted for publication March 15, 1995. Copyright © 1995 by Erian A. Armanios and Ashraf M. Badir. Published by the American Institute of Aeronautics and Astronautics, Inc., with permission.

*Associate Professor, School of Aerospace Engineering, Associate Fellow AIAA.

†Assistant Professor, Department of Engineering. Member AIAA.

where the average displacements along the coordinates are denoted by $U_i(x)$ ($i = 1, 2, 3$) and $\varphi(x)$ is the twist angle. The primes in Eq. (2) denote differentiation with respect to x . The function $g(s, x)$ added to the classical displacement field of extension, bending, and torsion represents the out-of-plane warping of the cross section and is determined from continuity of the displacement field and the vanishing of hoop stress resultant and constant shear flow.

The strain energy density Φ of two-dimensional anisotropic shell theory is associated with membrane behavior and can be expressed as

$$2\Phi = A_{11}(\gamma_{11})^2 + A_{22}(\gamma_{22})^2 + 4A_{66}(\gamma_{12})^2 + 2A_{12}\gamma_{11}\gamma_{22} + 4A_{16}\gamma_{11}\gamma_{12} + 4A_{26}\gamma_{22}\gamma_{12} \quad (3)$$

where A_{ij} ($i, j = 1, 2, 6$) are the laminate in-plane stiffnesses¹⁴ and $\gamma_{\alpha\beta}$ ($\alpha, \beta = 1, 2$) the in-plane tensorial strain components. The strain energy of the shell is given by

$$U = \int_0^L \oint \Phi \, ds \, dx \quad (4)$$

where the closed contour integral in Eq. (4) is performed over Γ .

The in-plane strains are related to the axial u_1 , tangential v_2 , and normal v displacement components associated with the curvilinear coordinate system x, s, ξ shown in Fig. 1 by

$$\begin{aligned} \gamma_{11} &= \frac{\partial u_1}{\partial x} \\ 2\gamma_{12} &= \frac{\partial u_1}{\partial s} + \frac{\partial v_2}{\partial x} \\ \gamma_{22} &= \frac{\partial v_2}{\partial s} + \frac{v}{R} \end{aligned} \quad (5)$$

The tangential and normal displacements are related to the Cartesian displacement components by

$$\begin{aligned} v_2 &= u_2 \frac{dy}{ds} + u_3 \frac{dz}{ds} \\ v &= u_2 \frac{dz}{ds} - u_3 \frac{dy}{ds} \end{aligned} \quad (6)$$

For the case of no internal pressure acting on the shell, the hoop stress resultant is negligibly small and may be ignored; thus,

$$N_{22} = \frac{\partial \Phi}{\partial \gamma_{22}} = 0 \quad (7)$$

Combine Eq. (7) with Eq. (3) to obtain

$$\gamma_{22} = -(1/A_{22})(A_{12}\gamma_{11} + 2A_{26}\gamma_{12}) \quad (8)$$

Substitute from Eq. (8) into Eq. (3), the strain energy density takes the form

$$2\Phi_1 = \min_{\gamma_{22}} 2\Phi = A(s)(\gamma_{11})^2 + 2B(s)\gamma_{11}\gamma_{12} + C(s)(\gamma_{12})^2 \quad (9)$$

where

$$\begin{aligned} A(s) &= A_{11} - \frac{(A_{12})^2}{A_{22}} \\ B(s) &= 2 \left[A_{16} - \frac{A_{12}A_{26}}{A_{22}} \right] \\ C(s) &= 4 \left[A_{66} - \frac{(A_{26})^2}{A_{22}} \right] \end{aligned} \quad (10)$$

Parameters $A(s)$, $B(s)$, and $C(s)$ represent the reduced axial, coupling, and shear stiffness, respectively. The shear flow N_{12} is constant and can be written as

$$N_{12} = \frac{\partial \Phi}{\partial (2\gamma_{12})} = \frac{1}{2}(B(s)\gamma_{11} + C(s)\gamma_{12}) \quad (11)$$

or

$$\gamma_{12} = \frac{2N_{12}}{C(s)} - \frac{B(s)}{C(s)}\gamma_{11} \quad (12)$$

Substitute for the strain in Eq. (12) in terms of the displacement components from Eqs. (5), (6), and (2) to get

$$\begin{aligned} \frac{\partial g}{\partial s} + \frac{2B(s)}{C(s)}g'(s, x) &= -r_n(s)\varphi' \\ &- \frac{2B(s)}{C(s)}[U_1' - y(s)U_2'' - z(s)U_3''] + \frac{4N_{12}}{C(s)} \end{aligned} \quad (13)$$

The projection of the position vector \mathbf{r} in the normal direction is denoted by r_n and expressed as

$$r_n = y \frac{dz}{ds} - z \frac{dy}{ds} \quad (14)$$

For a thin-walled slender beam whose dimensions satisfy Eq. (1), the rate of change of the displacement along the axial direction is much smaller than its rate of change along the circumferential direction. The coefficient of g' in Eq. (13) represents the ratio of in-plane extension-shear coupling stiffness $B(s)$ to the shear stiffness $C(s)$. For laminated composites $B(s)$ is less or of the same order as $C(s)$. Consequently, the second term in the left-hand side of Eq. (13) can be neglected relative to the first term.

The shear flow N_{12} is determined from the condition that the warping function $g(s, x)$ should be a single valued continuous function, i.e.,

$$\overline{\left(\frac{\partial g}{\partial s} \right)} = \frac{1}{l} \oint \frac{\partial g}{\partial s} ds = 0 \quad (15)$$

The integral in Eq. (15) is performed along the cross-sectional mid-plane closed contour Γ whose length is denoted by l . The overbar in Eq. (15) and in the subsequent derivation denotes averaging along the closed contour Γ . Substitute Eq. (13) into Eq. (15) to get

$$\begin{aligned} N_{12} &= \left[\frac{1}{4} \oint \frac{1}{C(s)} ds \right] \left\{ 2A_e \varphi'(x) + \oint \frac{2B(s)}{C(s)} \right. \\ &\quad \times [U_1'(x) - y(s)U_2''(x) - z(s)U_3''(x)] ds \left. \right\} \end{aligned} \quad (16)$$

where A_e is the enclosed area of the cross section given by

$$A_e = \frac{1}{2} \oint r_n ds = \frac{l}{2} \bar{r}_n \quad (17)$$

Integrate Eq. (13) and use Eq. (16) to obtain the warping function as

$$g(s, x) = G(s)\varphi'(x) + g_1(s)U_1'(x) + g_2(s)U_2''(x) + g_3(s)U_3''(x) \quad (18)$$

where

$$\begin{aligned} G(s) &= \int_0^s \left[\frac{2A_e}{l\bar{c}} c(\tau) - r_n(\tau) \right] d\tau \\ g_1(s) &= \int_0^s \left[b(\tau) - \frac{\bar{b}}{\bar{c}} c(\tau) \right] d\tau \\ g_2(s) &= - \int_0^s \left[b(\tau)y(\tau) - \frac{\bar{b}y}{\bar{c}} c(\tau) \right] d\tau \\ g_3(s) &= - \int_0^s \left[b(\tau)z(\tau) - \frac{\bar{b}z}{\bar{c}} c(\tau) \right] d\tau \end{aligned} \quad (19)$$

and

$$\begin{aligned} b(s) &= -[2B(s)/C(s)] \\ c(s) &= 1/C(s) \end{aligned} \quad (20)$$

The first term, $G(s)\varphi'$, in Eq. (18) is similar to the classical torsional-related warping, whereas the remaining three terms represent the out-of-plane warping due to uniform axial extension, $g_1(s)U_1'(x)$, due to bending about the z axis, $g_2(s)U_2''(x)$, and due to bending about the y axis, $g_3(s)U_3''(x)$. These three terms are significantly influenced by the material anisotropy and cross-sectional geometry. They vanish for materials that are either orthotropic or whose properties are antisymmetric relative to the shell middle surface.

Force-Deformation Relationships

The strain energy can be expressed in terms of the kinematic variables by substituting for γ_{11} from Eqs. (5), (2), and (18), and γ_{12} from Eqs. (12) and (16) into Eqs. (9) and (4) to get

$$U = \frac{1}{2} \int_0^L \{\delta\}^T [C]_{4 \times 4} \{\delta\} dx \quad (21)$$

where $\{\delta\}$ is 4×1 column matrix of kinematic variables defined as

$$\{\delta\}^T = \{U_1' \quad \varphi' \quad U_2'' \quad U_3''\} \quad (22)$$

The stiffness matrix $[C]$ is 4×4 symmetric matrix. Its components C_{ij} ($i, j = 1, 4$) are expressed in terms of the cross-sectional geometry and material properties as

$$\begin{aligned} C_{11} &= \oint \left(A - \frac{B^2}{C} \right) ds + \left\{ \left[\oint \left(\frac{B}{C} \right) ds \right]^2 / \oint \left(\frac{1}{C} \right) ds \right\} \\ C_{12} &= \left[\oint \left(\frac{B}{C} \right) ds / \oint \left(\frac{1}{C} \right) ds \right] A_e \\ C_{13} &= - \oint \left(A - \frac{B^2}{C} \right) z ds \\ &\quad - \left\{ \left[\oint \left(\frac{B}{C} \right) ds \oint \left(\frac{B}{C} \right) z ds \right] / \oint \left(\frac{1}{C} \right) ds \right\} \\ C_{14} &= - \oint \left(A - \frac{B^2}{C} \right) y ds \\ &\quad - \left\{ \left[\oint \left(\frac{B}{C} \right) ds \oint \left(\frac{B}{C} \right) y ds \right] / \oint \left(\frac{1}{C} \right) ds \right\} \\ C_{22} &= \left[1 / \oint \left(\frac{1}{C} \right) ds \right] A_e^2 \\ C_{23} &= - \left[\oint \left(\frac{B}{C} \right) z ds / \oint \left(\frac{1}{C} \right) ds \right] A_e \\ C_{24} &= - \left[\oint \left(\frac{B}{C} \right) y ds / \oint \left(\frac{1}{C} \right) ds \right] A_e \\ C_{33} &= \oint \left(A - \frac{B^2}{C} \right) z^2 ds \\ &\quad + \left\{ \left[\oint \left(\frac{B}{C} \right) z ds \right]^2 / \oint \left(\frac{1}{C} \right) ds \right\} \\ C_{34} &= \oint \left(A - \frac{B^2}{C} \right) y z ds \\ &\quad + \left[\oint \left(\frac{B}{C} \right) y ds \oint \left(\frac{B}{C} \right) z ds / \oint \left(\frac{1}{C} \right) ds \right] \\ C_{44} &= \oint \left(A - \frac{B^2}{C} \right) y^2 ds \\ &\quad + \left\{ \left[\oint \left(\frac{B}{C} \right) y ds \right]^2 / \oint \left(\frac{1}{C} \right) ds \right\} \end{aligned} \quad (23)$$

Parameters A , B , and C are defined in terms of the axial stiffness coefficients A_{ij} in Eq. (10).

Equations of Motion

The equations of motion of the undamped free vibration are derived using Hamilton's principle

$$\int_{t_1}^{t_2} \int_0^L \delta(K - U) dx dt = 0 \quad (24)$$

where t_1 and t_2 are arbitrary but fixed times and K is the kinetic energy density per unit length given by

$$K = \oint \int_{-h/2}^{+h/2} \frac{1}{2} \rho (\dot{u}_1^2 + \dot{u}_2^2 + \dot{u}_3^2) d\xi ds \quad (25)$$

where the dot denotes differentiation with respect to time. The material density is denoted by ρ . Substitute from Eq. (2) into Eq. (25) to get

$$\begin{aligned} K &= \oint \int_{-h/2}^{+h/2} \frac{1}{2} \rho \left[(\dot{U}_1 - y\dot{U}_2' - z\dot{U}_3' + \dot{g})^2 \right. \\ &\quad \left. + (\dot{U}_2 - z\dot{\varphi})^2 + (\dot{U}_3 + y\dot{\varphi})^2 \right] d\xi ds \end{aligned} \quad (26)$$

Based on inequalities (1), the underlined terms in Eq. (26) are of higher order in comparison with the remaining ones and, therefore, can be neglected. The resulting equations of motion in terms of the kinematic variables are

$$\begin{aligned} C_{11}U_1'' + C_{12}\varphi'' + C_{13}U_3''' + C_{14}U_2''' - m_e\ddot{U}_1 &= 0 \\ C_{12}U_1'' + C_{22}\varphi'' + C_{23}U_3''' + C_{24}U_2''' - I\ddot{\varphi} - S_z\ddot{U}_3 + S_y\ddot{U}_2 &= 0 \\ C_{13}U_1''' + C_{23}\varphi''' + C_{33}U_3'''' + C_{34}U_2'''' + S_z\ddot{\varphi} + m_e\ddot{U}_3 &= 0 \\ C_{14}U_1''' + C_{24}\varphi''' + C_{34}U_3'''' + C_{44}U_2'''' - S_y\ddot{\varphi} + m_e\ddot{U}_2 &= 0 \end{aligned} \quad (27)$$

The parameters associated with the inertia terms in Eqs. (27) are defined as

$$\begin{aligned} m_e &= \oint \rho h(s) ds \\ I &= \oint \rho (y^2 + z^2) h(s) ds \\ (S_y, S_z) &= \oint \rho (z, y) h(s) ds \end{aligned} \quad (28)$$

One of the members of each of the following pairs must be prescribed at the beam ends:

$$\begin{aligned} T \quad \text{or} \quad U_1, \quad M_x \quad \text{or} \quad \varphi, \quad M_y \quad \text{or} \quad U_3' \\ M_y' \quad \text{or} \quad U_3, \quad M_z \quad \text{or} \quad U_2', \quad M_z' \quad \text{or} \quad U_2 \end{aligned} \quad (29)$$

where T , M_x , M_y , and M_z are the axial force, twisting moment, and bending moments about the y and z axes, respectively. They are related to the kinematic variables by

$$\begin{Bmatrix} T \\ M_x \\ M_y \\ M_z \end{Bmatrix} = \begin{bmatrix} C_{11} & C_{12} & C_{13} & C_{14} \\ C_{12} & C_{22} & C_{23} & C_{24} \\ C_{13} & C_{23} & C_{33} & C_{34} \\ C_{14} & C_{24} & C_{34} & C_{44} \end{bmatrix} \begin{Bmatrix} U_1' \\ \varphi' \\ U_3'' \\ U_2'' \end{Bmatrix} \quad (30)$$

Applications

To illustrate the influence of coupling on the natural frequencies the theory is applied to two laminated composite configurations: the circumferentially uniform stiffness and the circumferentially asymmetric stiffness. These types of constructions have been considered in Refs. 4–13.

Assuming simple harmonic motion of the form

$$\mathcal{F}(x, t) = \bar{\mathcal{F}}(x)e^{i\omega t} \quad (31)$$

where \mathcal{F} is any state variable, the natural frequencies can be determined in closed form as follows.

Circumferentially Uniform Stiffness Configuration

For a CUS configuration, the axial, coupling, and shear stiffnesses A , B , and C are constant throughout the cross section as well as the thickness and material density. As a result, the stiffness coefficients $C_{13} = C_{14} = C_{23} = C_{24} = C_{34} = 0$ and the first moment of mass $S_y = S_z = 0$. The equations of motion reduce to

$$C_{11}U_1'' + C_{12}\varphi'' - m_c\ddot{U}_1 = 0 \quad (32)$$

$$C_{12}U_1'' + C_{22}\varphi'' - I\ddot{\varphi} = 0 \quad (33)$$

$$C_{33}U_3'''' + m_c\ddot{U}_3 = 0 \quad (34)$$

$$C_{44}U_2'''' + m_c\ddot{U}_2 = 0 \quad (35)$$

This configuration produces extension-twist coupling only.

For a cantilevered beam of length L , the natural frequencies of the extension-twist vibration modes described by Eqs. (32) and (33) are given by

$$\omega_n = n\pi\lambda/2L \quad (n = 1, 3, 5, \dots) \quad (36)$$

where

$$\lambda^2 = \frac{2\alpha}{\beta \pm \sqrt{\beta^2 - 4\alpha m_c I}} \quad (37)$$

with

$$\begin{aligned} \alpha &= C_{11}C_{22} - (C_{12})^2 \\ \beta &= C_{11}I + C_{22}m_c \end{aligned} \quad (38)$$

whereas the natural frequencies for bending about the y axis described by Eq. (34) is

$$\omega_n = k_n^2 \sqrt{C_{33}/m_c} \quad (39)$$

and bending about the z axis by

$$\omega_n = k_n^2 \sqrt{C_{44}/m_c} \quad (40)$$

where k_n in Eqs. (39) and (40) are the roots of the transcendental characteristic equation

$$\cos(kL) \cosh(kL) = -1 \quad (41)$$

and the first four roots are

$$\begin{aligned} k_1 L &= 1.87510, & k_2 L &= 4.69409 \\ k_3 L &= 7.85476, & k_4 L &= 10.99554 \end{aligned} \quad (42)$$

Consider the CUS box beam shown in Fig. 2. The beam has a $[20/-70/20/-70/20]_T$ layup and is made of T300/5208 graphite/epoxy material system with properties given in Ref. 15. A comparison of predictions from the present analytical model, with a finite element simulation are presented in Table 1. The first three natural frequencies due to vertical and horizontal free vibrations are provided together with the first two frequencies associated

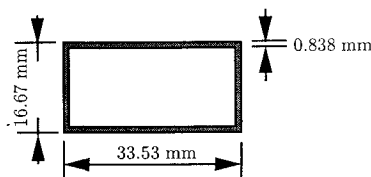


Fig. 2 Beam cross section.

Table 1 Comparison of frequencies (Hz) with stiffnesses based on NABSA

Mode	NABSA	Present	% Diff.
1VB	3.00	2.9585	-1.4
2VB	19.04	18.54	-2.6
3VB	54.65	51.92	-5.0
1HB	5.19	5.10	-1.7
2HB	32.88	31.98	-2.7
3HB	93.39	89.55	-4.1
1ET	180.32	177.05	-1.8
2ET	544.47	531.15	-2.4

Table 2 Cantilever geometry and properties

Width = 24.21 mm (0.953 in.)
Depth = 13.46 mm (0.53 in.)
Length = 762 mm (30.0 in.)
Ply thickness = 0.127 mm (0.005 in.)
$E_{11} = 142$ GPa (20.59 Msi)
$E_{22} = E_{33} = 9.8$ GPa (1.42 Msi)
$G_{12} = G_{13} = 6.0$ GPa (0.87 Msi)
$G_{23} = 4.83$ GPa (0.7 Msi)
$\nu_{12} = \nu_{13} = 0.42$, $\nu_{23} = 0.5$

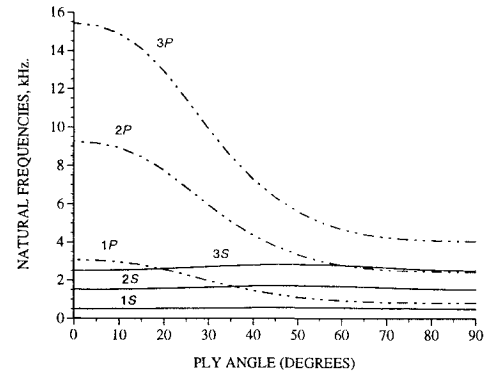


Fig. 3 Natural frequencies vs ply angle for the extension-twist coupled mode.

with extension-twist coupling mode. The vertical bending (VB), horizontal bending (HB), and extension-twist (ET) coupling modes are listed in the first column of Table 1. Numbers associated with these letters denote the respective mode. For example, n ET refer to the n th mode with coupled extension and twist. The nonhomogeneous anisotropic beam section analysis (NABSA) is a finite element model based on an extension of the work of Giavotto et al.¹⁶ This formulation calculates the cross-sectional properties of an anisotropic nonhomogeneous prismatic beam with constant material properties along its axis and subjected to loads applied at the end sections. A three-dimensional warping field is introduced to account for all possible deformations and linear strain-displacement relationships are adopted. The formulation is based on the principle of virtual work, and the finite element method is used to discretize the two-dimensional domain in terms of six global strain parameters, namely, extension, twist, and two bending and two transverse shear measures. The frequencies calculated from NABSA are provided by Hodges et al.¹⁵ The predictions of the present theory are in good agreement with NABSA.

The variation of natural frequencies with ply angle θ in a CUS cantilevered box beam with $[\theta]_6$ layup is plotted in Figs. 3 and 4. The cross-sectional dimensions and material properties are given in Table 2.

Figure 3 shows the variation of two types of modes. The first, denoted by nS ($n = 1, 2, 3$), corresponds to the n th mode that oscillates such that the twisting component has the same sign as the extensional component whereas the other, denoted by nP , corresponds to the n th mode which has an opposite sign. Figure 4 shows the variation of the vertical and horizontal bending modes denoted by VB and HB, respectively. Figures 3 and 4 show that ply angles

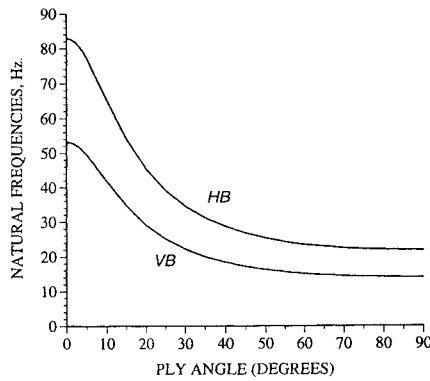


Fig. 4 Fundamental natural frequencies vs ply angle for the vertical (VB) and horizontal (HB) bending mode.

up to 60 deg have a significant influence on frequencies associated with extension-twist modes with opposite signs as well as vertical and horizontal bending modes.

Circumferentially Asymmetric Stiffness Configuration

For a CAS configuration, the axial stiffness A is constant throughout the cross section as well as the thickness and material density. Moreover, if the beam has a box cross section, the coupling stiffness B , in the opposite member is of opposite sign. As a result, the stiffness coefficients $C_{12} = C_{13} = C_{14} = C_{24} = C_{34} = 0$ and the first moment of mass $S_y = S_z = 0$. The equations of motion reduce to

$$C_{11}U_1'' - m_c\ddot{U}_1 = 0 \quad (43)$$

$$C_{22}\varphi'' + C_{23}U_3''' - I\ddot{\varphi} = 0 \quad (44)$$

$$C_{23}\varphi''' + C_{33}U_3'''' + m_c\ddot{U}_3 = 0 \quad (45)$$

$$C_{44}U_2'''' + m_c\ddot{U}_2 = 0 \quad (46)$$

This configuration produces twist-vertical bending coupling, as described by Eqs. (44) and (45). For a cantilevered beam of length L , the characteristic equation can be expressed in terms of the following cubic equation:

$$\alpha y^3 + \beta y^2 + \gamma y + \delta = 0$$

where

$$y = \lambda^2$$

$$\alpha = (C_{22}C_{33} - C_{23}^2)$$

$$\beta = C_{33}I\omega^2$$

$$\gamma = -C_{22}\omega^2 m_c$$

$$\delta = -\omega^4 I m_c$$

and λ represents the space domain eigenvalue. The associated roots and natural frequencies are solved for numerically by enforcing fixed-free boundary conditions.

The decoupled axial vibration frequency from Eq. (43) is

$$\omega_n = (n\pi/2L)\sqrt{C_{11}/m_c} \quad (n = 1, 3, 5, \dots) \quad (47)$$

The decoupled bending vibration about the z axis (horizontal vibration) is as given in Eqs. (40) and (42). Table 3 lists the natural frequencies of a CAS cantilevered box beam with $[30]_6$ layup. The cross-sectional dimensions and material properties are given in Table 2. The natural frequencies associated with twist-vertical bending coupling are denoted by nTV ($n = 1, 2, 3$), whereas nE and nHB denote extension and horizontal bending, respectively. It can be observed that the first six natural frequencies are associated with horizontal bending and coupled bending-twist modes. The lowest natural frequency corresponds to a bending-twist mode. As

Table 3 Natural frequencies (Hz) of a CAS cantilever beam with $[30]_6$ layups

Mode	Frequency
1E	1523.64
2E	4570.93
3E	7618.21
1TV	24.08
2TV	150.72
3TV	421.19
1HB	45.13
2HB	282.84
3HB	792.03

Table 4 Comparison of frequencies (Hz) with experimental data from Ref. 17

Material	Layup	Mode	Present	Ref. 17	% Diff.
Graphite/epoxy	$[30]_6$ CAS	1TV	19.92	20.96	-4.9
		2TV	124.73	128.36	-2.8
		1HB	37.62	38.06	-1.2
	$[45]_6$ CAS	1TV	14.69	16.67	-11.9
		2TV	92.02	96.15	-4.3
		1HB	25.13	29.48	-14.8
Kevlar®/epoxy	$[15]_6$ CUS	1VB	28.67	28.66	0.0
		1VB	34.23	30.66	11.7
		1VB	32.75	30.0	9.1
	$[0/30]_3$ CUS	1TV	10.73	10.65	-0.8
		2TV	67.20	61.46	9.3
		1TV	13.08	14.64	-10.7
Glass/epoxy	$[45]_2$ CAS	2TV	81.94	89.73	-8.9

expected, the natural frequencies associated with extension modes have relatively high numerical values.

A comparison of predictions from the present analytical model, with test data are presented in Table 4. The test data are based on Figs. 4, 6–8, 10, and 11 of Ref. 17. The details of the cantilever box beam geometry, layup, material properties, and wall thickness are listed in Table 1 of Ref. 17. Results show that the present theory is in good agreement with the test data.

Conclusion

An analysis for the free vibration of anisotropic thin-walled closed-section beams is developed. The theory accounts for arbitrary variations of stiffness along the cross section circumference. Closed-form expressions for the stiffness coefficients are derived and the contributions of material anisotropy is identified. The elastic coupling mechanism in thin-walled composite beam are evaluated for two configurations, one designed for extension-twist coupling and the other bending-twist coupling. The predicted results are compared with a finite element solution and test data. The derived closed-form expressions are suited for parametric design studies. An illustration is provided by investigating the influence of stacking angle on the frequencies associated with coupled vibration modes.

Acknowledgments

This work was supported by the U.S. Army Research Office under Grant DAAL03-92-G-03A0 and NASA Grant NAGW-2939. These supports are gratefully acknowledged. The authors would also like to acknowledge Matthew Greenman for his pertinent remarks regarding the CAS vibration response and the valuable discussions with D. Stefan Dancila.

References

- Hodges, D. H., "Review of Composite Rotor Blade Modeling," *AIAA Journal*, Vol. 28, No. 3, 1990, pp. 561–565.
- Reissner, E., and Tsai, W. T., "Pure Bending, Stretching, and Twisting of Anisotropic Cylindrical Shells," *Journal of Applied Mechanics*, Vol. 39, March 1972, pp. 148–154.
- Rehfield, L. W., "Design Analysis Methodology for Composite Rotor Blades," *Proceedings of the Seventh DoD/NASA Conference on Fibrous Composites in Structural Design*, AFWAL-TR-85-3094, June 1985, pp. (V(a)-1)–(V(a)-15).

⁴Atilgan, A. R., "Towards A Unified Analysis Methodology For Composite Rotor Blades," Ph.D. Dissertation, School of Aerospace Engineering, Georgia Inst. of Technology, Atlanta, GA, Aug. 1989.

⁵Rehfield, L. W., and Atilgan, A. R., "Shear Center and Elastic Axis and Their Usefulness for Composite Thin-Walled Beams," *Proceedings of the American Society For Composites, Fourth Technical Conference* (Blacksburg, VA), 1989, Technomic, Lancaster, PA, pp. 179-188.

⁶Rehfield, L. W., Atilgan, A. R., and Hodges, D. H., "Nonclassical Behavior of Thin-Walled Composite Beams with Closed Cross Sections," *Journal of the American Helicopter Society*, Vol. 35, No. 2, 1990, pp. 42-50.

⁷Smith, E. C., and Chopra, I., "Formulation and Evaluation of an Analytical Model for Composite Box-Beams," *Proceedings of the AIAA/ASME/ASCE/AHS/ASC 31st Structures, Structural Dynamics, and Materials Conference* (Long Beach, CA), AIAA, Washington, DC, 1990, Pt. 2, pp. 759-782.

⁸Smith, E. C., and Chopra, I., "Formulation and Evaluation of an Analytical Model for Composite Box-Beams," *Journal of the American Helicopter Society*, Vol. 36, No. 3, 1991, pp. 23-35.

⁹Chandra, R., Stemple, A. D., and Chopra, I., "Thin-Walled Composite Beams under Bending, Torsional, and Extensional Loads," *Journal of Aircraft*, Vol. 27, No. 7, 1990, pp. 619-626.

¹⁰Nixon, M. W., "Analytical and Experimental Investigations of Extension-Twist-Coupled Structures," M.S. Thesis, George Washington Univ., Washington, DC, May 1989.

¹¹Kosmatka, J. B., "Extension-Bend-Twist Coupling Behavior of Thin-Walled Advanced Composite Beams with Initial Twist," *Proceedings of the AIAA/ASME/ASCE/AHS/ASC 32nd Structures, Structural Dynamics, and Materials Conference* (Baltimore, MD), AIAA, Washington, DC, 1991, Pt. 2, pp. 1037-1049.

¹²Badir, A. M., "Analysis of Advanced Thin-Walled Composite Structures," Ph.D. Thesis, School of Aerospace Engineering, Georgia Inst. of Technology, Atlanta, GA, Feb. 1992.

¹³Berdichevsky, V., Armanios, E., and Badir, A., "Theory of Anisotropic Thin-Walled Closed-Cross-Section Beams," *Composite Engineering* (Special Issue), Vol. 2, Nos. 5-7, 1992, pp. 411-432.

¹⁴Vinson, J. R., and Sierakowski, R. L., *The Behavior of Structures Composed of Composite Materials*, Martinus-Nijhoff, Dordrecht, The Netherlands, p. 54.

¹⁵Hodges, D. H., Atilgan, A. R., Fulton, M. V., and Rehfield, L. W., "Free-Vibration Analysis of Composite Beams," *Journal of the American Helicopter Society*, Vol. 36, No. 3, 1991, pp. 36-47.

¹⁶Giavotto, V., Borri, M., Mantegazza, P., Ghiringhelli, G., Carmashi, V., Maffioli, G. C., and Mussi, F., "Anisotropic Beam Theory and Applications," *Computers and Structures*, Vol. 16, Nos. 1-4, 1983, pp. 403-413.

¹⁷Chandra, R., and Chopra, I., "Experimental-Theoretical Investigation of the Vibration Characteristics of Rotating Composite Box Beams," *Journal of Aircraft*, Vol. 29, No. 4, 1992, pp. 657-664.